JOURNAL OF DENTAL HEALTH & ORAL RESEARCH

e-ISSN 3050-9432

Journal of Dental Health and Oral Research

ATHENAEUM SCIENTIFIC PUBLISHERS

Research Article

Finite Element Study of Upper Molar Distalization Using a Vertical Beveled Rectangular Attachment: Influence of Buccal Surface Positioning

Gilberto Salas[1*]

[1]Medical Stomatologist, Digital Orthodontist, Private Practice in Alcoy, Spain

***Correspondence author:** Gilberto Salas Medical Stomatologist, Digital Orthodontist, Private Practice in Alcoy, Spain; E-mail: gilbertosalas42@gmail.com

Citation: Salas G. Finite Element Study of Upper Molar Distalization Using a Vertical Beveled Rectangular Attachment: Influence of Buccal Surface Positioning. J Dental Health Oral Res. 2025;6(2):1-12.

https://doi.org/10.46889/JDHOR.2025.6229

Received Date: 02-08-2025

Accepted Date: 18-08-2025

Published Date: 25-08-2025

Abstract

Background: Molar distalization in adult patients using clear aligners remains a biomechanical challenge, particularly regarding the efficiency of force transmission and the control of secondary movements. Attachment positioning may significantly influence tooth movement.

Methods: Three 3D finite element models of an upper first molar with a 1 mm PET-G aligner were developed, differing only in the mesial, central or distal placement of a vertical beveled rectangular attachment. Dental displacement, contact forces and Periodontal Ligament (PDL) stress were evaluated using Autodesk Fusion FEA.

Results: Central attachment placement produced the greatest distal displacement (0.314 mm), while mesial placement generated the lowest PDL stress (0.150 MPa) despite slightly higher contact force (1.2 N). All models exhibited ~2° coronal tipping.

Conclusions: Attachment position influences movement magnitude and biomechanical efficiency. Mesial placement may optimize stress distribution, while Autodesk Fusion provides an accessible platform for digital orthodontic biomechanical analysis.

Keywords: Molar Distalization; Clear Aligners; Finite Element Simulation; Orthodontic Attachments; Digital Orthodontics; Aligner Stiffness

Abbreviations

CBCT: Cone Beam Computed Tomography; PDL: Periodontal Ligament; PET-G: Polyethylene Terephthalate Glycol; FEA: Finite Element Analysis

Nomenclature

k: Structural stiffness (N/mm); F: Applied force (N); δ: Displacement (mm); E: Young's modulus (MPa); ν: Poisson's ratio; L: Transmission length (mm); b: Effective width of contact (mm); h: Thickness of the aligner (mm)

Introduction

The emergence of clear aligner therapy and particularly the molar distalization protocols introduced by Invisalign®, has significantly improved the predictability of molar distalization, enabling non-extraction treatments for premolars (although third molars are still often extracted) [1]. Early clinical reports described tooth displacements of 0.25-0.33 mm per aligner; however, these lacked rigorous experimental validation [2]. Since then, considerable research has been devoted to understanding the biomechanical parameters governing this technique.

Simon, et al., demonstrated reliable molar distalization of 0.20 mm per stage and estimated an average force of 1.1 N, although they observed extreme variations ranging from 1 to 15 N between aligners [3,4]. Subsequent *in-vitro* studies by Kohda, et al., revealed that the initial force depends heavily on both the aligner material and the degree of activation [5]. Barbagallo, et al., reported that a 0.5 mm activation with a 0.8 mm polyurethane aligner could generate an initial insertion force of 5.1 N [6].

Gao, et al., analyzed the biomechanical effects of upper molar distalization using clear aligners, comparing step distances of 0.250 mm and 0.130 mm and found that the difference between horizontal and vertical attachments did not significantly affect molar displacement or stress distribution [7]. Using Finite Element Analysis (FEA), their results showed that simultaneous distalization of two molars with a reduced step produced results similar to those obtained by distalizing a single molar.

Li, et al., examined the orientation of the rectangular attachment, finding that a vertical placement at 90° resulted in purer distalization, while a 135° placement favored molar distalization combined with intrusion and a 45° placement promoted distalization with extrusion [8]. Recent studies by Li, et al., also emphasize the need to correct coronal tipping by incorporating an overcorrection of 6° [9]. Kuguoglu, et al., explained that placing two attachments one on the mesial/buccal surface and another on the lingual/distal surface makes upper molar distalization more predictable [10]. Furthermore, the difficulty of distalizing second molars in the presence of third molars has been highlighted.

Traversa, et al., analyzed the mechanical behavior of clear aligners during initial insertion using a physical model that did not simulate the Periodontal Ligament (PDL) and treated teeth as rigid bodies [11]. The recorded forces, which peaked at 16.97 N during molar distalization, reflected initial values without biological dissipation and involved aligners extending up to 2 mm subgingivally.

The central research question in the present study was how the magnitude and direction of orthodontic forces vary during upper molar distalization when a vertical beveled rectangular attachment is placed at the mesial, central or distal regions of the buccal surface. The simulation focused on the immediate insertion of the aligner and the initial coronal tipping movement produced. Our findings indicated that placing the attachment at the central region of the buccal surface generated a more efficient force vector producing greater distal displacement with reduced tipping and intrusion compared to mesial or distal placements, although the quantitative differences were modest. This aligns with recent evidence from Kuguoglu, et al., who demonstrated that attachment positioning significantly influences the predictability of molar distalization [10].

In contrast to the rigid-body approach of Traversa, et al., the present study employed a parametric model incorporating a viscoelastic PDL, as described by Toms, et al. [11,12]. This allowed a more realistic estimation of effective forces applied at the root level. Using an insertion force of 7 N and an aligner margin positioned 1 mm from the gingival line, our results reflected a biomechanical response closer to physiological conditions. These findings highlight the importance of integrating PDL simulation to improve the predictive accuracy of biomechanical analyses in clear aligner therapies [12-14].

This study utilized a finite element model of an upper molar with a PET-G aligner (1 mm thickness) positioned 1 mm from the PDL to quantify the forces generated in each attachment configuration and to test the proposed hypothesis, thereby providing objective criteria for digital treatment planning in adult molar distalization cases [15]. Additionally, the study was conducted using Autodesk Fusion software, leveraging its accessible CAD and FEA simulation modules to facilitate incorporation into clinical orthodontic diagnostic workflows. Finally, this study posits that attachment positioning influences not only the magnitude of dental displacement but also the efficiency of force transmission to the periodontal biological system. The primary objective was to biomechanically compare, through finite element simulation, three potential placements of the vertical beveled rectangular attachment on the buccal surface of the upper first molar, evaluating their effects on displacement, contact force and stress distribution within the periodontal ligament.

Methodology

Geometric Model

The present study was conducted using Cone-Beam Computed Tomography (CBCT) data from a patient scheduled for distal movement of the right upper first molar. The DICOM dataset was imported into 3D Slicer (v. X.X), where the region of interest comprising the molar, surrounding alveolar bone and periodontal structures was segmented [16,17]. Two full-scale sagittal slices were selected to serve as reference planes for subsequent modeling.

The contours of both cortical and trabecular bone were manually delineated and a maxillary bone model was generated using the Loft tool in Autodesk Fusion 360, ensuring anatomical fidelity to the CBCT dataset [18]. The crown and root of the molar

were modeled using Fusion 360's Create Form tool, which allows organic surface construction based on the CBCT Canvas images, thereby preserving the original dimensions and morphology.

The Periodontal Ligament (PDL) was modeled in Meshmixer by applying the Select → Offset function at 0.25 mm to the exported tooth geometry from Fusion 360, producing an irregular surface consistent with the physiological PDL space [19]. This PDL model was then re-imported into Fusion 360, aligned and subjected to Boolean subtraction from the parametric maxillary bone model to create the final assembly.

The center of mass of the tooth was calculated automatically within the software, based on the assigned material properties. The maxillary gingiva was not modeled, as it was considered not to influence the biomechanical outcomes of the present simulation (Fig. 1).

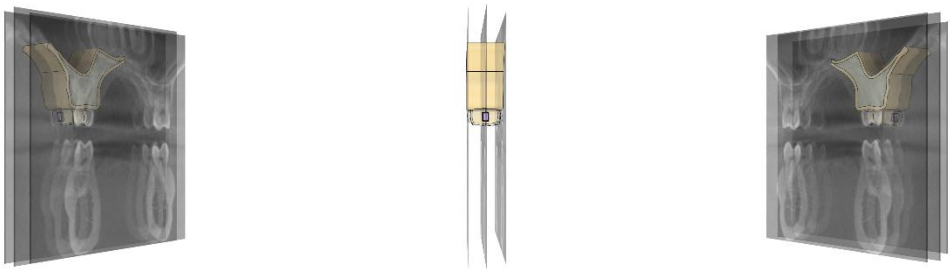

Figure 1: Workflow for segmentation and 3D reconstruction of the right upper first molar, alveolar bone and periodontal ligament from CBCT data. A) Isometric mesial view; B) orthogonal sagittal view showing PDL–root alignment; C) isometric distal view.

From three cross-sections of the CBCT, a parametric model was constructed by lofting operations, incorporating appropriate cortical and alveolar bone thicknesses within the Autodesk Fusion CAD environment, at a 1:1 scale. The crown and root of the molar were modeled directly onto the Canvas images extracted from the CBCT slices, employing the organic form creation tool in Fusion 360. Similarly, the Periodontal Ligament (PDL) was generated with a uniform thickness of 0.25 mm. The aligner cap was modeled using the same software, simulating a PET-G structure with a 1 mm thickness, positioned 1 mm away from the PDL. A vertical beveled rectangular attachment measuring 2.0 × 1.5 mm was designed on the buccal surface of the molar, following biomechanical criteria for aligner force optimization described in previous finite element analyses of attachment design (Fig. 2).

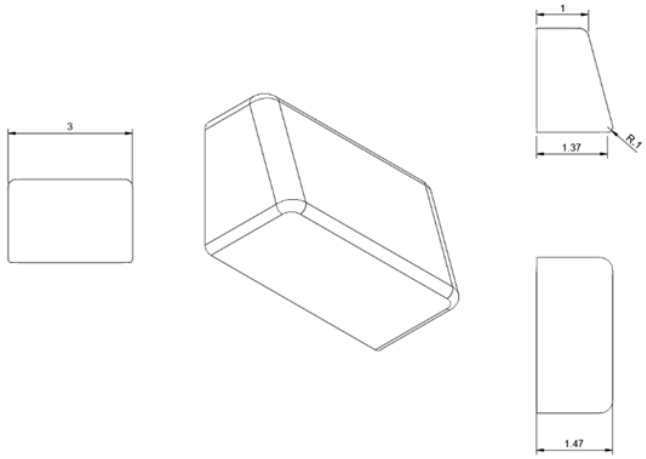

Figure 2: Technical design of a vertical beveled rectangular attachment for aligner biomechanics. Dimensions: 2.0 × 1.5 mm, positioned on the buccal surface of the right upper first molar with the bevel oriented gingivally to enhance aligner engagement and distalizing force control [17,20].

Three duplicates of the parametric model were created, modifying only the attachment position (mesial, central or distal) to isolate its biomechanical effect. The model variations are shown below (Fig. 3) [21].

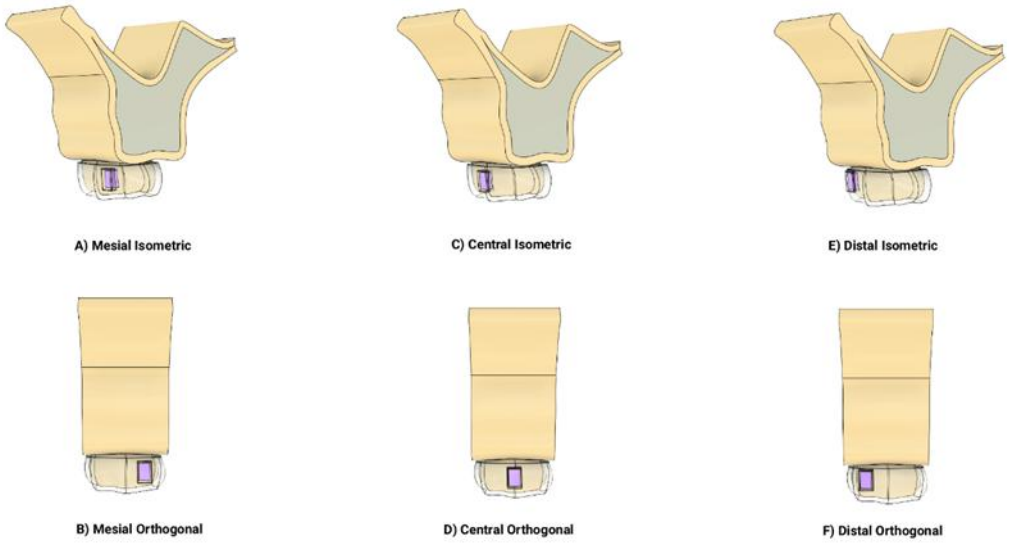

Figure 3: Upper first molar models with beveled rectangular attachment in mesial (A, B), central (C, D) and distal (E ,F) buccal positions. A, C, E: isometric views; B, D, F: orthogonal views.

Material Properties

Linear elastic constants were adopted from the experimental database of Kim, et al., for dentoalveolar tissues. In the linear regime, the Young's modulus (E) and Poisson's ratio (ν) values were as follows [9]:

- Cortical bone: 13,700 MPa / 0.30
- Trabecular bone: 1,370 MPa / 0.30
- Tooth: 20,000 MPa / 0.30
- Attachment resin: 12,500 MPa / 0.30
- PET-G aligner: 2,050 MPa / 0.46
- Periodontal ligament (PDL): 0.40 MPa / 0.45

Boundary Conditions and Loading

The bone complex was anchored by fixed constraints at the lateral sinus wall and the zygomatic process to simulate *in-vivo* skeletal support. Contacts between the attachment, aligner and tooth were defined as "bonded" with a friction coefficient $\mu = 0.20$. Similarly, the tooth–PDL and PDL–bone interfaces were defined as bonded, representing the Sharpey fiber insertions [22].

The clinical activation was simulated by applying a 0.3 mm distal translation to the aligner within the digital setup. The resulting force was compared against the experimentally reported value of 7 N for 1 mm PET-G aligners [23].

Unlike previous model versions, the PDL was modeled here as a linear elastic material ($E = 0.40$ MPa; $\nu = 0.45$) to facilitate direct comparison with data from Traversa, et al., who used the same assumption in a multidental mechanical analysis without FEA simulation. Therefore, no local mesh refinement nor nonlinear Newton-Raphson algorithms were required [9]. A linear static solver was sufficient to capture the small displacements (<0.35 mm) analyzed. All other components (alveolar bone, cortical bone, aligner and tooth) were modeled as linear, elastic, isotropic and homogeneous materials, appropriate for the low-magnitude stress changes contemplated in this study.

Meshing and Numerical Solution

Each model variant was meshed with triangular surface elements, which are particularly suitable for accurately representing the curvature of the PDL and dental interfaces. This type of planar mesh offers advantages for biomechanical simulations requiring

precise adaptation to complex anatomical geometries, such as tooth roots, PDL interfaces and beveled structures, minimizing surface distortions, as reported in similar finite element analyses of clear aligners [24].

Subsequently, the models were meshed into 3D linear tetrahedral elements (4-node tetrahedrons), as natively handled by the Fusion 360 meshing engine, balancing computational efficiency with adequate resolution for small displacement analyses. The final model consisted of 86,587 nodes and 51,814 elements. A localized refinement of ≤10% was applied at the PDL–tooth interface to ensure better capturing of stress and deformation gradients, critical in this biologically sensitive region. The simulation was considered converged when the displacement change between two consecutive iterations was below 5%, indicating numerical stability and a sufficiently accurate solution for the clinical orthodontic context of the study [25].

Complete Simulation Workflow

The procedure, illustrated below, followed this sequence:

CBCT acquisition → 3D Slicer segmentation → Fusion 360 CAD modeling → Triangular meshing → Material and contact assignment → FEA solution (Fusion 360) → Post-processing of von Mises stress and displacement maps. Under this methodology, three geometrically identical models were generated, differing only in attachment positioning. This allowed comparison, under controlled conditions, of the magnitude and direction of the molar distalization force generated by each configuration. The simulation workflow is detailed below (Fig. 4) [26].

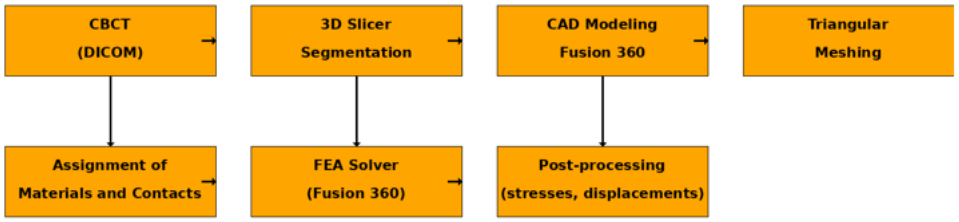

Figure 4: Workflow diagram for finite element simulation: CBCT acquisition, 3D segmentation, CAD modeling, triangular meshing, material and contact assignment, FEA solution and post-processing of stress and displacement results.

Results

Numerical simulations revealed that small variations in the position of the beveled rectangular attachment significantly modified both the magnitude and quality of the molar distalization movement. The displacement maps for the three attachment positions are shown below (Fig. 5).

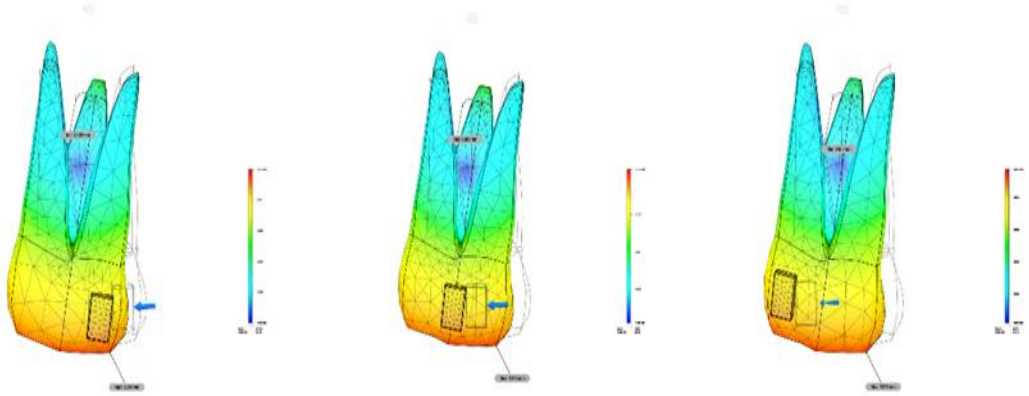

Figure 5: Displacement maps of the upper first molar with beveled rectangular attachment at mesial (A), central (B) and distal (C) positions. Color scale shows displacement magnitude (mm) under identical activation (0.3 mm distal movement, 7 N load).

Quantitative comparison of maximum displacement values among the three attachment positions using a one-way Analysis of Variance (ANOVA) revealed a statistically significant effect ($F = 83.67$, $p < 0.0000001$). Tukey's post hoc test showed that all pairwise comparisons were significant ($p < 0.001$), confirming that even small positional changes produce measurable differences in distalization magnitude (Table 1) [27].

Comparison	Mean difference (mm)	p-adj	Significant
Distal vs Central	0.020	<0.001	Yes
Distal vs Mesial	0.040	<0.001	Yes
Central vs Mesial	0.020	<0.001	Yes

Table 1: Tukey's post hoc comparisons of maximum displacement (mm) between attachment positions.

Model 1 (Distal Attachment Position)

The center of the mesiobuccal cusp displaced by 0.300 mm.

A comparative summary of displacement magnitudes across the three models is presented below (Fig. 6).

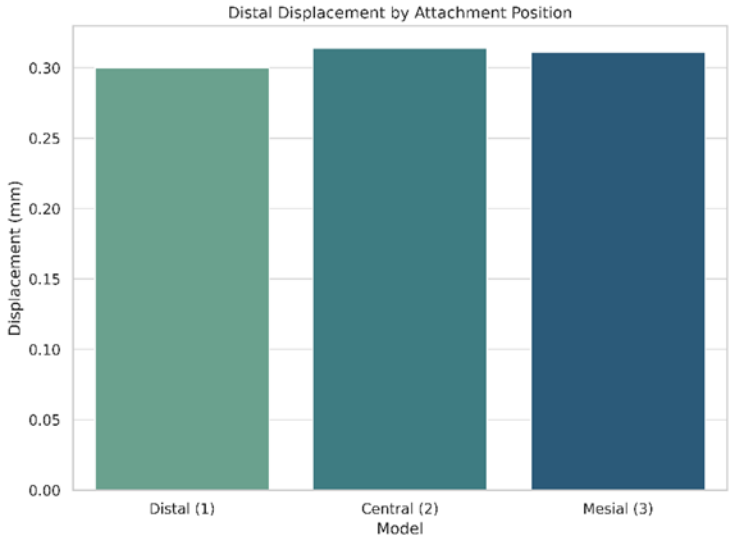

Figure 6: Comparison of displacement magnitudes for the upper first molar across the three attachment positions: (M1) distal, (M2) central and (M3) mesial.

The force vector did not pass through the tooth's center of resistance, generating approximately 2° of coronal tipping. The center of rotation was located internally on the palatal root surface.

The von Mises stress distribution in the periodontal ligament (PDL) for this model is illustrated below (Fig. 7).

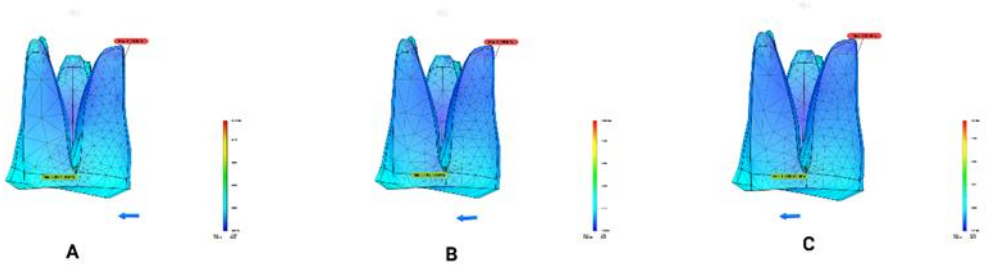

Figure 7: Von Mises stress distribution in the Periodontal Ligament for the Upper First Molar with the beveled rectangular attachment placed at (A) Mesial, (B) Central and (C) Distal positions.

The von Mises stress in the PDL for the first molar reached 0.205 MPa.

A comparative summary of von Mises stress levels across the three models is shown below (Fig. 8).

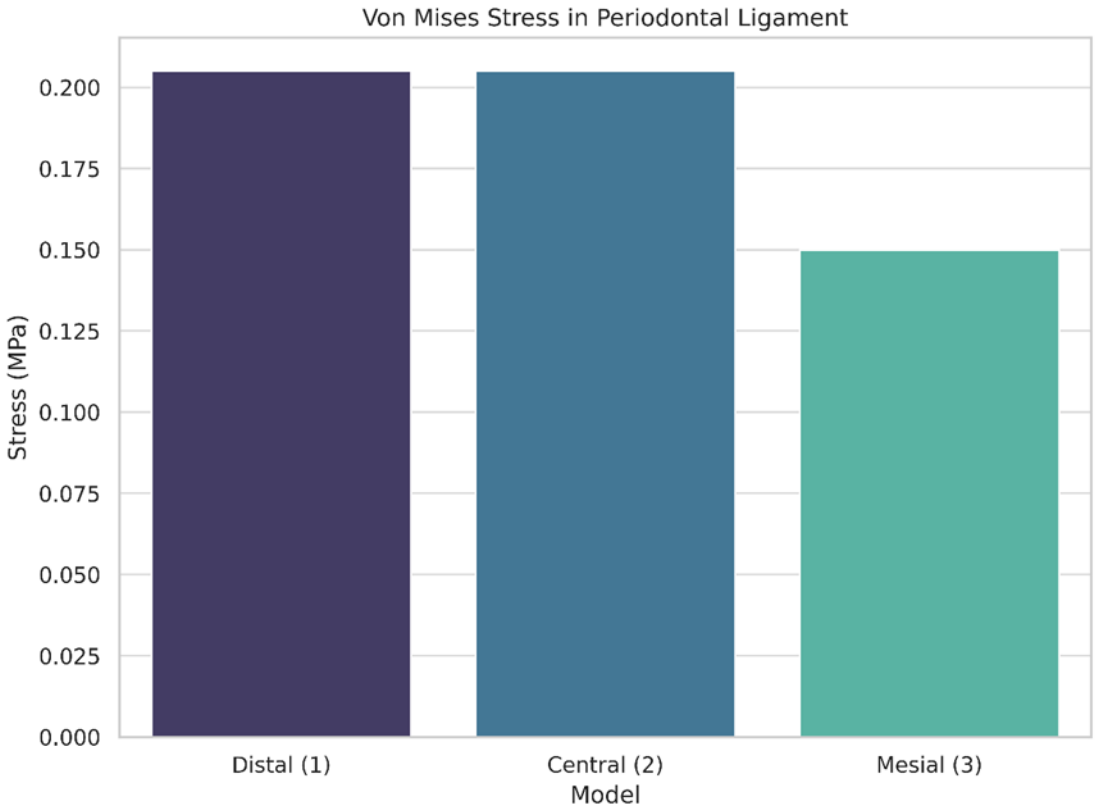

Figure 8: Comparison of von Mises stress magnitudes in the periodontal ligament for the upper first molar across the three attachment positions: (M1) distal, (M2) central and (M3) mesial.

The distribution of contact force varied depending on the attachment position, concentrating primarily on the active face of the attachment (Fig. 9).

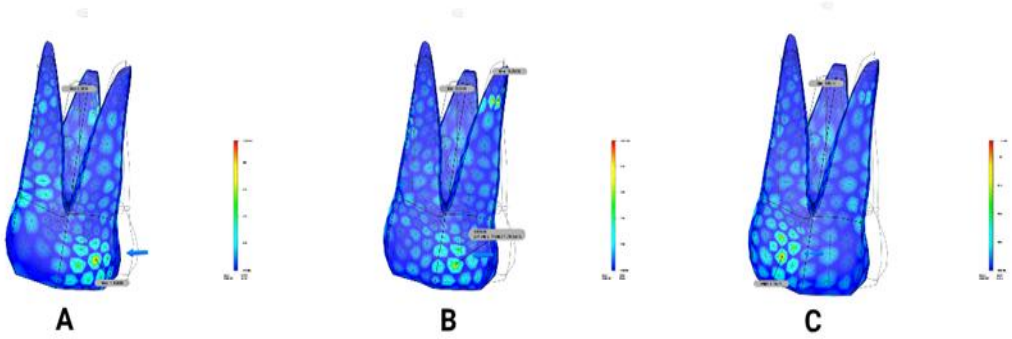

Figure 9: Contact force distribution for mesial (A), central (B) and distal (C) loading conditions. In the central position (B), the mesiobuccal root showed the highest contact force, while the distal–buccal surface with the attachment had markedly lower magnitudes.

The comparative magnitudes of contact force across the three models are summarized below (Fig. 10).

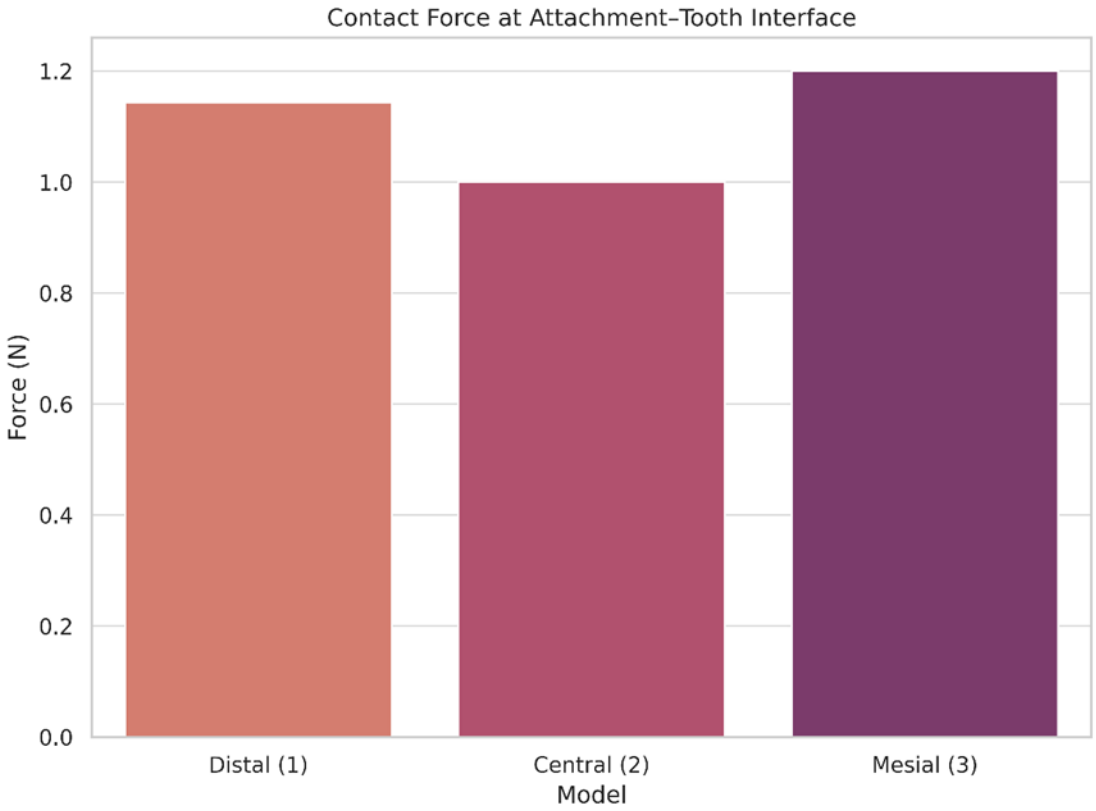

Figure 10: Comparison of contact force magnitudes at the attachment–aligner interface for the upper first molar across the three attachment positions: (M1) distal, (M2) central and (M3) mesial.

Model 2 (Central Attachment Position)

The displacement of the mesiobuccal cusp was 0.314 mm.

A coronal tipping of 2° was also observed, with the center of rotation located internally on the palatal root surface.

The von Mises stress in the PDL was 0.206 MPa, with the maximum stress concentrated at the apex of the mesiobuccal root. The contact force at the attachment–crown interface was 1.1 N.

Model 3 (Mesial Attachment Position)

The displacement reached 0.311 mm, with approximately 2° of coronal tipping. The center of rotation was likewise located on the palatal root. In this case, the von Mises stress in the PDL was 0.150 MPa. The recorded contact force at the attachment–crown interface was 1.2 N.

Simulated Force vs. Contact Force

In the context of finite element analysis studies, it is crucial to distinguish between simulated force and contact force:

- Simulated force refers to the theoretical load introduced in the digital setup—in this case, a 0.3 mm distal activation applied to the aligner. It represents the intended clinical movement
- Contact force is the actual force resulting from the interaction between surfaces (aligner–attachment, tooth–PDL), calculated by the software based on local geometry, material properties, friction and system deformation. Unlike simulated force, it is not prescribed but emerges as an output of the analysis

Comparing these forces allows for the evaluation of the system's biomechanical efficiency.

An activation force of 7 N may not effectively translate into distalization if the attachment does not seat correctly or if slack is present in the aligner fit. Therefore, analyzing contact forces at critical areas is essential for validating the clinical behavior of the aligner and optimizing its design.

Structural Stiffness of the Aligner

The biomechanical efficiency of an aligner depends on its ability to generate controlled and sustained forces. Structural stiffness is defined as the ratio of applied force to resulting displacement and is expressed by [28]:

$k = F / \delta$

Where:

- k is stiffness (N/mm)
- F is applied force (N)
- δ is resulting displacement (mm)

In orthodontic aligners, stiffness is also influenced by geometric and material properties.

The schematic profile of the aligner illustrating the parameters h (aligner thickness) and b (effective contact width) used in the stiffness calculation is shown below (Fig. 11).

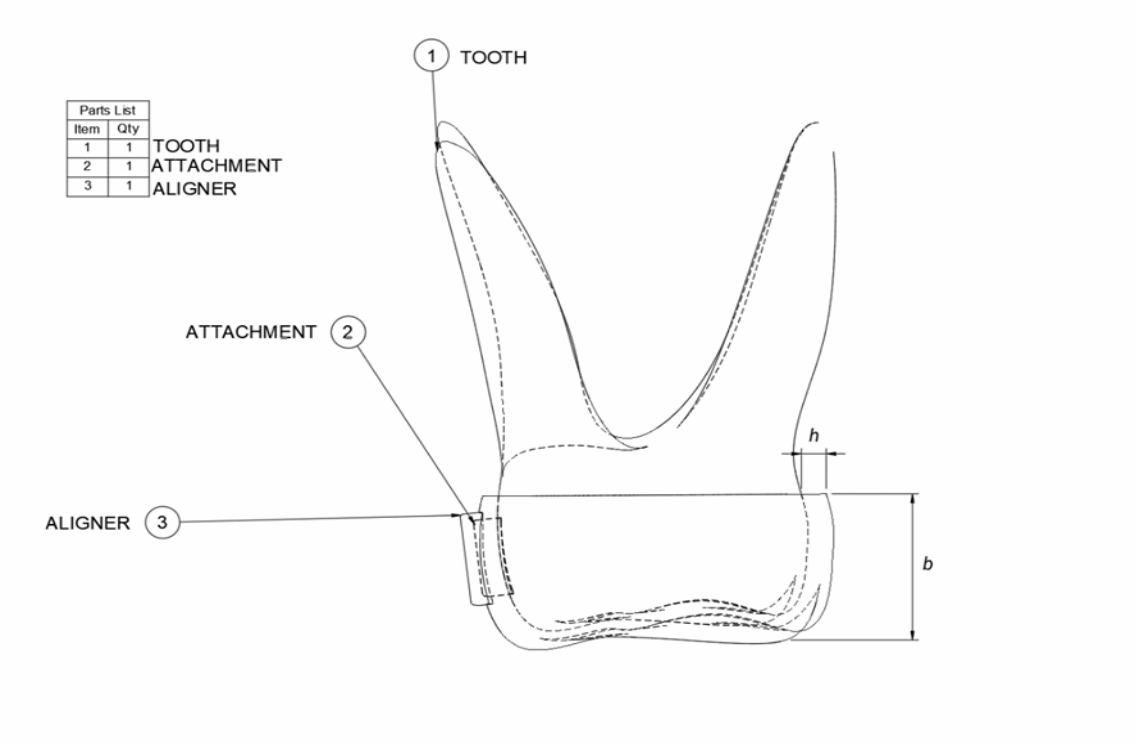

Figure 11: Exploded schematic of the upper first molar showing the main components used in stiffness and force calculations: (1) Tooth (crown and root), (2) Buccal attachment and (3) Aligner. Aligner thickness (h) and contact width (b) are entered into the stiffness calculation model [33].

Based on thin-plate theory, structural stiffness can be expressed as [29]:

$k = (E \cdot b \cdot h^3) / (12 \cdot (1 - \nu^2) \cdot L)$

where:

- E is Young's modulus
- ν is Poisson's ratio
- L is transmission length

This relationship implies that small increases in aligner thickness (h) significantly enhance stiffness and thus the generated force. Conversely, higher values of Poisson's ratio (ν) or transmission length (L) decrease stiffness, promoting smoother movements.

Clinical Applications

From a clinical perspective, greater aligner stiffness is desirable during phases requiring high control, such as molar distalization or intrusion. However, excessive stiffness may cause discomfort or adverse biological responses. Thus, carefully adjusting material and thickness parameters is crucial to ensure forces remain within a biologically safe and clinically effective range.

The mathematical formulation of stiffness offers a solid quantitative tool for the design and customization of aligners, enabling adaptation to specific patient needs and enhancing the predictability of digital orthodontic treatments. All necessary parameters for each aligner and movement can be calculated using a programmed calculator [30]. These results provide an objective basis for analyzing how attachment positioning can influence not only the magnitude of dental movement but also its biomechanical quality. The clinical and biomechanical implications of these findings are discussed below.

Discussion

All three attachment configurations produced molar distalization movements within the clinically expected range for a 0.3 mm activation, confirming their viability in clinical scenarios. Notably, the mesial position combined a relatively higher contact force with the lowest von Mises stress in the periodontal ligament, suggesting a more favorable biomechanical distribution. This could reduce the risk of periodontal overload and enhance treatment safety, highlighting the importance of evaluating not only movement magnitude but also stress distribution when choosing attachment configurations [30].

There are notable differences with previous studies. Simon, et al., estimated that a force of 1.1 N was sufficient to achieve a displacement of 0.2 mm, whereas Li, et al., proposed ranges between 8 and 9 N [4,8].

In the present study, an intermediate value of 7 N was adopted, aligning more closely with the physiological values reported by Traversa, et al., who also incorporated models featuring a periodontal ligament and more realistic anatomical structures [8]. Unlike the physical model used by Traversa which omitted the PDL and recorded force peaks up to 16.97 N our model, which integrated the PDL, produced more contained and clinically compatible force values [9].

The force values obtained in the present finite element model were in line with those reported by Traversa, et al., who analyzed clear aligner biomechanics using a physical model without periodontal ligament representation [9]. Their findings also placed the effective forces transmitted to the tooth within a physiological range, supporting the validity of our simulated loading conditions.

This convergence supports the clinical validity of our FEA results. Ye, et al., also demonstrated that a verified FEA model of clear aligners predicted aligner-tooth gaps and strain fields with an R^2 of 0.99 compared to experimental measurements, confirming that digitally simulated models can reliably reproduce force magnitudes while offering added insight into internal stress patterns and rotational tendencies that *in-vitro* experiments cannot capture [25].

From a clinical perspective, one of the most relevant findings was the immediate coronal tipping of approximately 2° observed in all models. This inclination is consistent with the angular overcorrection strategies recommended by Li, et al., who propose programming up to 6° of tipping to counteract distal tipping and promote more controlled bodily movement [9].

Our data reinforce the utility of vertical attachments as auxiliary control surfaces and emphasize the effectiveness of Class II elastics, especially when applied through precision cuts, to enhance anchorage and reduce adverse effects on anterior teeth.

Nevertheless, the present study is limited to a single-tooth model and does not account for interactions with anchorage systems or adjacent teeth. Moreover, the simulation was performed under quasi-static conditions, without considering force degradation over time or interindividual variability in periodontal ligament response. Dynamic friction effects and micro-movements from speech or mastication were also not incorporated.

These findings contribute novel evidence to a relatively unexplored area: how the three-dimensional positioning of the attachment affects not only the magnitude of dental movement but also the internal biological loading patterns. This approach promotes a more comprehensive view of clear aligner therapy and may represent a turning point in the design of more personalized and efficient treatment protocols.

Limitations

This study is based on a controlled, single-tooth finite element model simulating the immediate effects of a 0.3 mm distal activation. While providing valuable biomechanical insights, it does not account for interproximal contacts, full-arch anchorage effects or long-term material fatigue phenomena. Additionally, while the periodontal ligament was modeled as a linear elastic material to facilitate computational convergence, its real biomechanical behavior is viscoelastic, nonlinear and anisotropic.

Future studies incorporating hyperelastic models could further enhance the accuracy of force transmission simulations and better represent biological responses during orthodontic loading. Consequently, the findings should be interpreted within the context of first-stage aligner activations and isolated molar distalization and further clinical validation *in-vivo* is necessary to corroborate these results.

Clinical Implications and Future Research Directions

Within the parameters of this finite element analysis, mesial attachment placement showed a more favorable stress distribution in the periodontal ligament without reducing distalization magnitude, suggesting a potential biomechanical advantage for cases where periodontal load minimization is a priority. The structural stiffness of the aligner emerged as a critical factor in force transmission, underscoring the need to consider both material and geometric properties during digital treatment planning.

Conclusion

Attachment position affects biomechanics in molar distalization; the central position gives the greatest displacement, while the mesial offers the lowest PDL stress. The mesial configuration, despite higher contact force, showed lower PDL stress, indicating greater efficiency and reduced biological risk. Using 1 mm PET-G aligners with vertical rectangular attachments and Class II elastics enables controlled distalization with minimal extrusion when attachment placement and stiffness are optimized. Fusion 360 is a practical tool for planning and training in digital orthodontics.

Conflict of Interest
There are no conflicts of interest that may have influenced the research, authorship or publication of the article.

Financial Disclosure
No financial support was received for the writing, editing, approval or publication of this manuscript.

Ethical Statement
This project was exempt from IRB review as it did not qualify as human subject research under federal regulations.

References

1. Boyd RL, Miller RJ, Vlaskalic V. The Invisalign system in adult orthodontics: Mild crowding and space closure cases. J Clin Orthod. 2000;34(9):203-12.
2. Schupp W, Haubrich J, Neumann I. Class II correction with the Invisalign system. J Clin Orthod. 2010;44(1):28-35.
3. Simon M, Schwarze J, Jung BA, Bourauel C. Treatment outcome and efficacy of an aligner technique regarding incisor torque, premolar derotation and molar distalization. BMC Oral Health. 2014;14:68.
4. Simon M, Keilig L, Schwarze J, Jung BA, Bourauel C. Forces and moments generated by removable thermoplastic aligners: Incisor torque, premolar derotation and molar distalization. Am J Orthod Dentofacial Orthop. 2014;145(5):728-36.
5. Kohda N, Iijima M, Muguruma T, Brantley WA, Ahluwalia KS, Mizoguchi I. Effects of mechanical properties of thermoplastic materials on the initial force of thermoplastic appliances. Angle Orthod. 2013;83(3):476-83.
6. Barbagallo L, Shen G, Jones AS, Swain MV, Petocz P, Darendeliler MA. A novel pressure film approach for determining the force imparted by clear removable thermoplastic appliances. Ann Biomed Eng. 2008;36(2):335-41.
7. Gao J, Guo D, Zhang X, Cheng Y, Zhang H, Xu Y, et al. Biomechanical effects of different staging and attachment designs in maxillary molar distalization with clear aligner: A finite element study. Prog Orthod. 2023;24(1):43.
8. Li J, Wang X, Chen Y, Zhang L. Effect of attachment orientation and vertical force components on upper second molar distalization with clear aligners: A finite element analysis. Orthod Craniofac Res. 2025;28(2):123-32.
9. Li J, Yang Y, Tang Z. Biomechanical analysis of the effect of aligner overtreatment on molar distalization with clear aligners: A finite-element study [preprint]. Research Square. 2024.
10. Kuguoglu A, Akarsu-Guven B. Evaluation of the effects of the third molar on distalization and the effects of attachments on distalization and expansion with clear aligners: Three-dimensional finite element study. Korean J Orthod. 2025;55(1):69-81.

11. Traversa F, Chavanne P, Mah J. Biomechanics of clear aligner therapy: assessing the influence of tooth position and flat trimline height in translational movements. Orthod Craniofac Res. 2024.
12. Toms SR, Eberhardt AW. A nonlinear finite element analysis of the periodontal ligament under orthodontic tooth loading. Am J Orthod Dentofacial Orthop. 2003;123(6):657-65.
13. Kang F, Wu Y, Cui Y. The displacement of teeth and stress distribution on periodontal ligament under different upper incisors proclination with clear aligner in cases of extraction: A finite element study. Prog Orthod. 2023;24:38.
14. Inan A, Gonca M. Effects of aligner activation and power arm length and material on canine displacement and periodontal ligament stress: A finite element analysis. Prog Orthod. 2023;24:40.
15. Rojas GA, García-Melo JI, Aristizábal JS. Finite element simulation of biomechanical effects on periodontal ligaments during maxillary arch expansion with thermoformed aligners. J Funct Biomater. 2025;16:143.
16. Fedorov A, Beichel R, Kalpathy-Cramer J. 3D Slicer as an image computing platform for the quantitative imaging network. Magn Reson Imaging. 2012;30(9):1323-41.
17. Barone S, Paoli A, Razionale A, Savignano R. Design of customised orthodontic devices by digital imaging and CAD/FEM modelling. In: Proceedings of the International Conference on Computer Graphics Theory and Applications (GRAPP 2016). Rome: SCITEPRESS. 2016:44-52.
18. Autodesk Fusion 360 [software]. San Rafael (CA): Autodesk Inc.
19. Meshmixer [software]. San Rafael (CA): Autodesk Inc.
20. Ravera S, Castroflorio T, Garino F, Daher S, Cugliari G, Deregibus A. Maxillary molar distalization with aligners in adult patients: A multicenter retrospective study. Prog Orthod. 2016;17:12.
21. Kuguoglu A, Akarsu-Guven B. Evaluation of the effects of the third molar on distalization and the effects of attachments on distalization and expansion with clear aligners: Three-dimensional finite element study. Korean J Orthod. 2025;55(1):69-81.
22. Savignano R, Valentino R, Razionale AV, Michelotti A, Barone S, D'Antò V. Biomechanical effects of different auxiliary-aligner designs for the extrusion of an upper central incisor: A finite element analysis. J Healthc Eng. 2019;2019:1-9.
23. Gómez JP, Pen FM, Martínez V, Giraldo DC, Cardona CI. Initial force systems during bodily tooth movement with plastic aligners and composite attachments: A three-dimensional finite element analysis. Angle Orthod. 2015;85(3):454-60.
24. Türk T, Kucukkaraca E. Biomechanical evaluation of attachment and trimline modifications in maxillary molar distalization using clear aligners. Appl Sci. 2025;15(11):5873.
25. Ye N, Brown BE, Mantell SC, Heo YC, Larson BE, Fok AS. Validation of finite element models for orthodontic aligners. J Mech Behav Biomed Mater. 2022;134:105404.
26. Cai Y, Yang X, He B. Finite element method analysis of the periodontal ligament in mandibular canine movement with transparent tooth correction treatment. BMC Oral Health. 2015;15:106.
27. Mao B, Tian Y, Li J, Zhou Y. Expansion rebound deformation of clear aligners and its biomechanical influence: A three-dimensional morphologic analysis and finite element analysis study. Angle Orthod. 2023;93(5):572-9.
28. Albertini P, Staderini E, Patini R, Gallenzi P, Giuntoli F, Paganelli C, et al. Mechanical properties of thermoplastic materials for clear aligners: A systematic review. Materials (Basel). 2022;15(15):5409.
29. Rossini G, Schiaffino M, Parrini S, Sedran A, Deregibus A, Castroflorio T. Upper second molar distalization with clear aligners: A finite element study. Appl Sci. 2020;10(21):7739.
30. Domagalski Ł, Kowalczyk I. Optimization and analysis of plates with a variable stiffness distribution in terms of dynamic properties. Materials (Basel). 2025;18(9):2150.
31. Rossini G, Schiaffino M, Parrini S, Sedran A, Deregibus A, Castroflorio T. Upper second molar distalization with clear aligners: A finite element study. Appl Sci. 2020;10(21):7739.
32. Salas G. Aligners Stiffness Calculator. Ortodoncia Digital Gilberto Salas. [Last accessed on : August 18, 2025] https://www.ortodonciadigitalgilbertosalas.com/calculadora-de-la-rigidez-alineadores